

An alternative model for ultra-high pressure in the Svartberget Fe-Ti garnet-peridotite, Western Gneiss Region, Norway

JOHANNES C. VRIJMOED^{1,*}, YURI Y. PODLADCHIKOV¹, TORGEIR B. ANDERSEN¹ and EBBE H. HARTZ^{1,2}

¹ Physics of Geological Processes (PGP), University of Oslo, PO Box 1048, Blindern, 0316 Oslo, Norway

*Corresponding author, e-mail: j.c.vrijmoed@fys.uio.no

² Aker Exploration AS, PO Box 580, Sentrum, 4003 Stavanger, Norway

Abstract: The previously reported “Fe-Ti type” garnet-peridotite is located in the northern part of the well known ultra-high pressure (UHP) area of the Western Gneiss Region (WGR) in Norway. Primary spinel stable up to only 2.0 GPa at 800 °C coexists with Caledonian ultra-high pressure (4.0 GPa at 800 °C) grt-cpx-opx-ol assemblages in the Svartberget garnet-peridotite. The body is cut by a conjugate set of metasomatic fractures filled dominantly with diamond-bearing garnet-phlogopite-websterite (5.5 GPa at 800 °C) and garnetite. Single zircon U-Pb dating suggests metamorphic growth of zircon in the garnetite at 397.2 ± 1.2 Ma, either coinciding or predating an initial phase of leucosomes formation at 397–391 Ma. Field observations, major and trace elements, mineral-chemistry, polyphase inclusions including microdiamond, coupled with ⁸⁷Sr/⁸⁶Sr ratios in clinopyroxene and whole rock ranging from 0.73 to 0.74, suggest that the Svartberget garnet-peridotite was infiltrated by melts/fluids from the host-rock gneiss during the Caledonian UHP event. Present observations in the WGR document a regional metamorphic gradient increasing towards the NW, and structures in the field can account for the exhumation of the (U) HP rocks from ~2.5 to 3 GPa. Assuming lithostatic pressures the diamond-bearing Svartberget peridotite body must have come from a burial depth of more than 150 km. However, there is a lack of observable structures in the field to explain exhumation from extreme UHP conditions (5.5 GPa or more) to normal HP-UHP conditions (2.5–3 GPa), which are common pressures calculated from eclogites in western parts of the WGR. Because of the regional and mostly coherent metamorphic gradient across the WGR terrain, it is difficult to account for local extreme pressure excursions such as documented from within the Svartberget peridotite. We introduce here a conceptual model to explain the main features of the Svartberget body. During burial and heating, rocks surrounding the peridotite start to melt but surrounding non-molten rocks confine the space and pressure builds up. When pressure is high enough, conjugate brittle shear fractures develop in the peridotite. Melt (or supercritical fluid) that has the same pressure (5.5 GPa) as the surrounding gneiss can flow in as soon as fractures propagate into the peridotite. This supercritical fluid is now highly reactive and metasomatism takes place at UHP conditions along the fractures capturing micro inclusions of diamond while growing. Finally the lithosphere holding the overpressurised gneiss constrained breaks due to formation of large-scale fractures in the crust and decompression melting starts. Modelling using finite-element method (FEM) shows that melting of the gneiss results in pressure variations when gneiss is ten to hundred times weaker than surroundings and peridotite enclave. These pressure variations can be up to several GPa and are qualitatively similar to observations in the field.

Key-words: ultra-high pressure metamorphism, overpressure, Western Gneiss Region, micro-diamond, Fe-Ti garnet-peridotite.

1. Introduction

The problem of exhumation of ultra-high pressure rocks in the Western Gneiss Region in Norway has been challenging since the first UHP discoveries in the WGR (Smith, 1984). The WGR is well known for its occurrences of HP to UHP rocks, mainly found as eclogite and peridotite boudins and lenses and more rarely within felsic gneisses. The HP-UHP metamorphism (HPM-UHPM) was associated with the continental collision between Baltica and Laurentia around 400 Ma ago (Torsvik *et al.*, 1996). Present observations document a regional metamorphic gradient increasing towards

the NW (Labrousse *et al.*, 2004), and structures in the field can account for the exhumation of the (U) HP rocks from ~2.5 to 3 GPa. Three distinct “UHPM domains” have been identified, predominantly along the NW margin of the WGR (Root *et al.*, 2005). The UHP locality in the northernmost UHPM domain, called Svartberget, is an Fe-Ti type garnet-peridotite that is crosscut by Caledonian phl-grt-websterite and garnetite veins. Peak *P-T* estimates for the crosscutting veins reach about 5.5 GPa at a temperature of 800 °C, supported by the presence of microdiamond (Vrijmoed *et al.*, 2008). Assuming lithostatic pressures, the diamond-bearing rocks at Svartberget in the northernmost UHP

domain of the WGR must have come from a burial depth of more than 150 km. Advanced numerical and analogue models exist to explain how UHP rocks can be created at great depth and be exhumed to the surface (Gerya *et al.*, 2002, 2008; Warren *et al.*, 2008). These models predict pressures up to 5 GPa resulting from deep (150–200 km) burial of crustal rocks in a subduction channel. The models simulate the path that UHP rocks travelled from the original position at shallow depths down to extreme depth and back to its present final position of UHP domains at the surface.

However, there is a lack of observable structures in the field to explain exhumation from extreme UHP conditions (5.5 GPa or more) to normal HP-UHP conditions (2.5–3 GPa), which are common pressures calculated from eclogites in western parts of the WGR. Because of the regional and mostly coherent metamorphic gradient across the WGR terrain, it is difficult to account for local extreme pressure excursions such as documented from within the Svartberget peridotite. We discuss a completely different conceptual model and present results of calculations using FEM to check the feasibility of our conceptual model.

A profile in the southern part of the WGR is shown in Fig. 1. To the east we have the Proterozoic intact Baltica basement with the Caledonian nappes on top separated from the basement by major extensional structures. Going to the west the first HP rocks in the form of eclogites are found 42 km away from the extensional contact between the Jotun nappe. Based on field measurements the vertical distance between the nappes and the first eclogites is 23 km. Assuming a hinterland dip of 30 to 60° during the Caledonian collision, a vertical distance of 26.5–46 km can be reached. Allowing for a conservative 10 km of erosion, the present geometry suggests original crustal thicknesses to be 58.5 km to a maximum of 70 km for the first appearance of eclogites. Eclogite-facies temperature estimates are around 650–700 °C and give a reasonable geotherm between 9–12 °C/km. The HP rocks to the north are positioned structurally below the rocks to the south where the profile was shown. Going towards the coast, structures are positioned deeper than 70 km, reaching a depth of about 90 km. This estimate already stretches the observed structural data and we take therefore 90 km as the maximum depth estimated from structural reconstructions.

In this paper we will focus our study on the Svartberget peridotite body that yield *P-T* estimates in crosscutting grt-phl-websterite veins of 5.5 GPa at 800 °C (Vrijmoed *et al.*, 2006). Assuming lithostatic pressures and an average rock density of 3000 kg/m³ this would indicate that the Svartberget rocks were at a depth of 165 km. This depth is not supported by structural field data and we therefore consider an alternative. The alternative is to consider the possibility of having variations in pressure rather than a continuous homogeneous pressure gradient from surface to depth. Pressure variations must have existed on the grain scale to preserve coesite in strong host minerals such as garnet and zircon (Gillet *et al.*, 1984; van der Molen & van Roermund, 1986; Sobolev *et al.*, 1994; Zhang, 1998; Ye *et al.*, 2001; Perrillat *et al.*, 2003; O'Brien & Ziemann, 2008). Also on a larger scale, for example in volcanic

systems, it seems possible that the lithosphere is able to sustain pressures above lithostatic long enough to be recorded in minerals (Blundy *et al.*, 2006). This leads us to the interesting idea that perhaps such a situation in which pressures, considerably higher than lithostatic might be sustained on a time scale that allows minerals to record these pressures. This might solve the discrepancy between the depth estimated by assuming lithostatic pressure and the lack of structures in the field to account for burial to the large depths. It has been stated before that in confined space pressures derived from inclusions may not have depth significance (Zhang, 1998). Our idea is that partial melting of felsic gneiss in a confined space is a possible mechanism to account for the UHP and large pressure variations recorded in the Svartberget peridotite located in the WGR. This concept has been proposed for the first time for UHP rocks in Greenland (Hartz *et al.*, 2007; Dabrowski *et al.*, 2008), to explain how UHP rocks can be created in the overriding plate. After introducing the available data on the Svartberget peridotite we propose a model to explain the data and combine this with numerical modelling to test the feasibility of the conceptual model.

2. Data

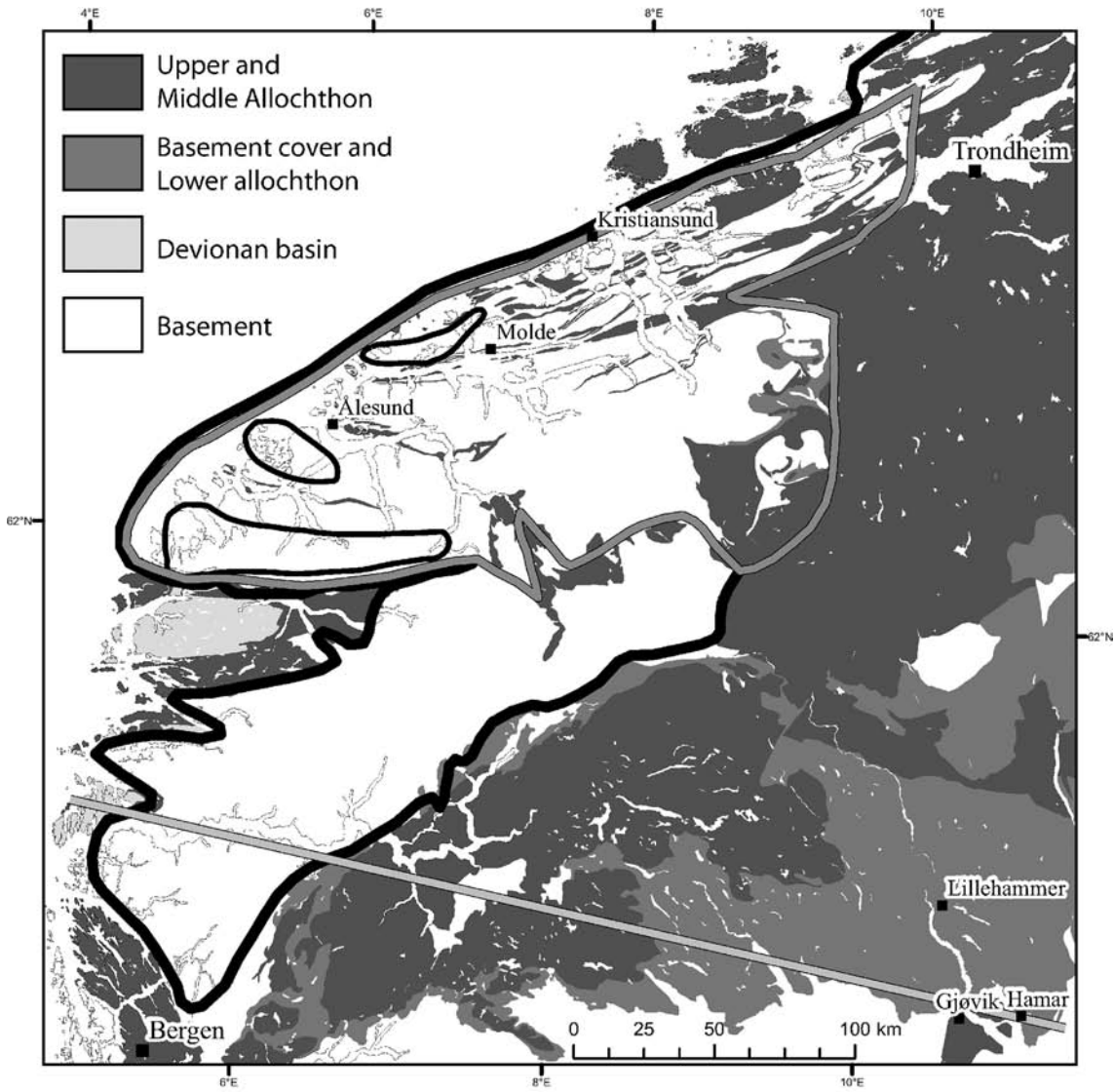
The Svartberget peridotite is crosscut by a conjugate set of fractures along which metasomatic zoning developed due to the infiltration of supercritical fluids from the surrounding gneisses at UHP conditions at the end of the Caledonian orogeny. Data on the Svartberget peridotite presented before (Vrijmoed *et al.*, 2006, 2008; Vrijmoed, 2008) will be shortly repeated below to facilitate the explanation of our model.

2.1. Field

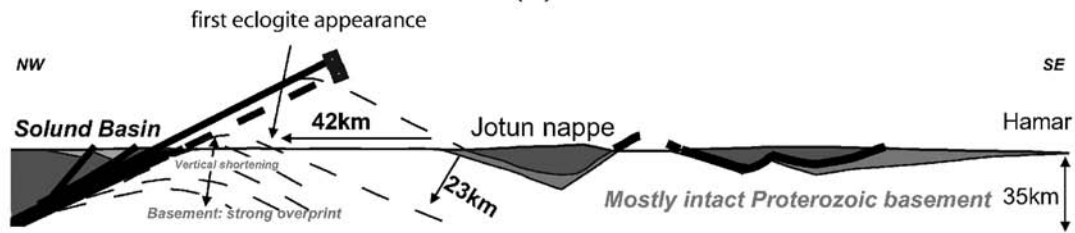
Aerial photographs and field measurements reveal that the dominant fractures crosscutting the Svartberget peridotite form a conjugate set indicative of brittle deformation. Figure 2 shows a map of structures, an aerial photograph and stereographic projection of measured fracture planes.

The aerial photograph is an orthophoto, which means that the distances and angles are corrected for distortion due to the angle at which the photo was taken. It can be seen from the photograph that the Svartberget peridotite is broken in pieces and many of the fractures cut each other with a ~60° angle. A detailed mapping was done by measuring all pieces and blocks of the peridotite and for suitable fracture planes orientation and dip were measured. The strike of these fracture planes is shown in Fig. 2a, and the azimuth and dip are presented in a stereographic projection in Fig. 2c. The angle between the averages of the two dominant groups of fractures is 55°. From the aerial photo and field measurements it is clear there is also a minor amount of fractures oriented differently (plotted grey in Fig. 2c).

The lithology in the fractures is typically diamond-grade phl-grt-websterite with a core of garnetite (Fig. 3).



(a)



(b)

Fig. 1. (a) Map of West Norway showing the WGR, intact Proterozoic basement with cover and Caledonian nappes (Lower, Middle and Upper Allochthon) and Devonian old red sandstone basins on top. The area that is overprinted by Caledonian HP and UHP metamorphism is indicated by the thick grey line. The thick black line indicates the location of major extensional contacts and outlines approximately the WGR. Domains in which UHP evidence is documented are outlined by thin black lines along the west coast. The light grey line indicates location of the profile below (modified after Tucker *et al.*, 2004). (b) Profile through the southern part of the WGR showing the main structures and distances between major contacts. It shows how the intact Proterozoic basement in the east is overlain by Caledonian nappes more to the west and ultimately is overprinted by HP metamorphism. In the east, separated by major extensional contacts (thick black lines), the Caledonian nappes with Devonian basins on top are shown. From this figure it can be concluded that the structures can explain a vertical distance of at most 70 km including 10 km erosion for the first appearance of eclogites in the east. More to the north structures might explain a maximum depth of 90 km.

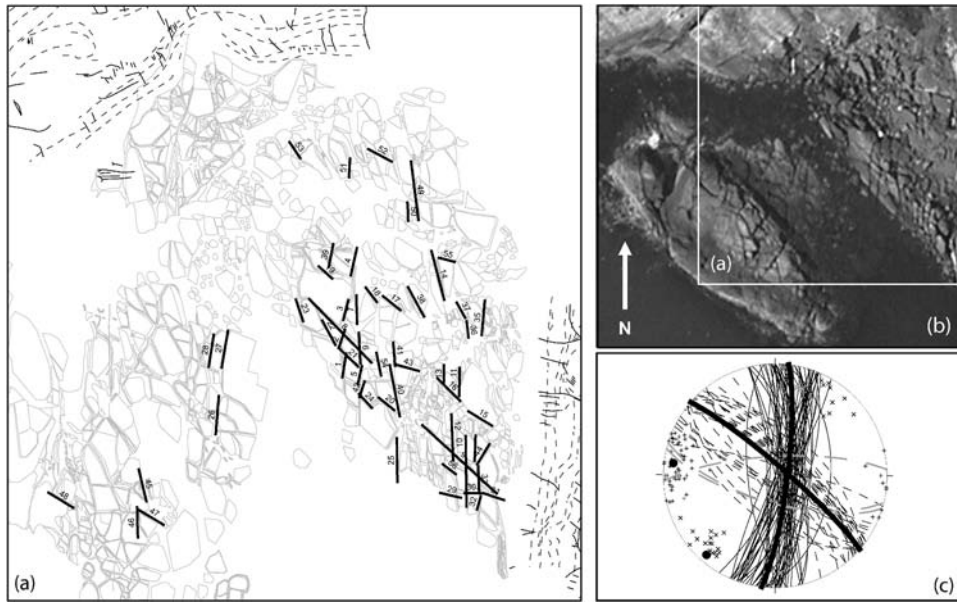


Fig. 2. (a) Structural map showing representative measurements of the fractures crosscutting the Svartberget peridotite. Numbers are for identification of the fractures. The background light grey lines show outlines of individual peridotite blocks and veins in fractures. Thin black lines indicate late brittle fractures (joints), and the foliation in surrounding gneiss is indicated by thin black broken lines. The regular pattern characteristic of conjugate sets of fractures can already be seen from the outlines of mapped blocks, aerial photograph shown in (b) and selected measured fractures highlighted in black. (c) Orientation of selected measured fractures in (a) plotted as poles and great circles in a stereographic projection. Thick black lines show the average of two major fracture sets (thin black lines for fractures 1–7, 10–14, 25–28, 32–36, 39–42, 46, 49, 51, 54, and thin black broken lines for fractures 8, 9, 15–22, 24, 47, 52, 55, 56) and their poles in filled black circles. A minor fracture set is also shown in light grey broken lines (fractures 29–31). The figures show how the two main sets of fractures form a conjugate pair that is characteristic for brittle shear fractures.

This applies to all fractures shown in Fig. 2c. More detailed observations reveal a total of 11 different lithological zones along the fractures, and contacts between the individual zones are sharp (Vrijmoed, 2008). Field observations, major and trace elements, mineral chemistry, polyphase inclusions including microdiamond, coupled with $^{87}\text{Sr}/^{86}\text{Sr}$ ratios in clinopyroxene and whole rock ranging from 0.73 to 0.74, suggest that the Svartberget grt-peridotite was infiltrated by melts/fluids from the host-rock gneiss during the Caledonian UHP event (Vrijmoed *et al.*, in prep). Peak P - T estimates for grt-websterite samples yield 5.5 GPa at 800 °C based on the Al-in-opx barometer of Brey & Köhler (1990) and micro inclusions of diamond were found by Vrijmoed *et al.* (2008). The peridotite has low-pressure primary spinel stable up to a pressure of 2.0 GPa at a temperature of 800 °C preserved, while geothermobarometry on opx-grt-cpx assemblages yield pressures around 4.0 GPa and temperatures around 800 °C. This issue will be discussed in a future paper (Vrijmoed, in prep.) where it is suggested, based on field evidence, that pressure variations may have existed during UHPM. Here we will provide a concept of a mechanism behind such pressure variations. The main observations that are important for this paper is that the phl-grt-websterites in the fractures yield much higher pressure estimates than the peridotite, which itself contains remnants of early low-pressure spinel.

Migmatitic quartzo-feldspathic biotite-amphibole gneisses surround the peridotite. These are ductily deformed with abundant leucosomes and eclogite-amphibolite boudins (Fig. 3). Leucosomes are present as several centimeter thick slivers on a small scale throughout the whole extent of the outcrop, up to 50 cm wide layers on the scale of several tens of meters. The composition of the leucosomes and melanosomes in the gneiss is typical for migmatites formed during the partial melting of metapelites, by comparison with well-known examples of migmatites (Bea *et al.*, 1994). Sillimanite and occasionally tiny garnets can be observed in the gneiss.

2.2. Timing

Garnet-clinopyroxene mineral pairs yield a Sm-Nd cooling age of 393 ± 3 Ma for the peridotite and 381 ± 6 Ma for the websterite, suggesting that the grt-cpx assemblages in the Svartberget body formed during the UHPM of the Caledonian orogeny. Details of the dating are discussed in Vrijmoed *et al.* (2006). The grt-cpx mineral separates were taken from the same samples that were used for the P - T estimates and that yielded UHPM conditions.

There is a number of steps that can be recognized within the present database of ages (Vrijmoed *et al.*, in prep.):

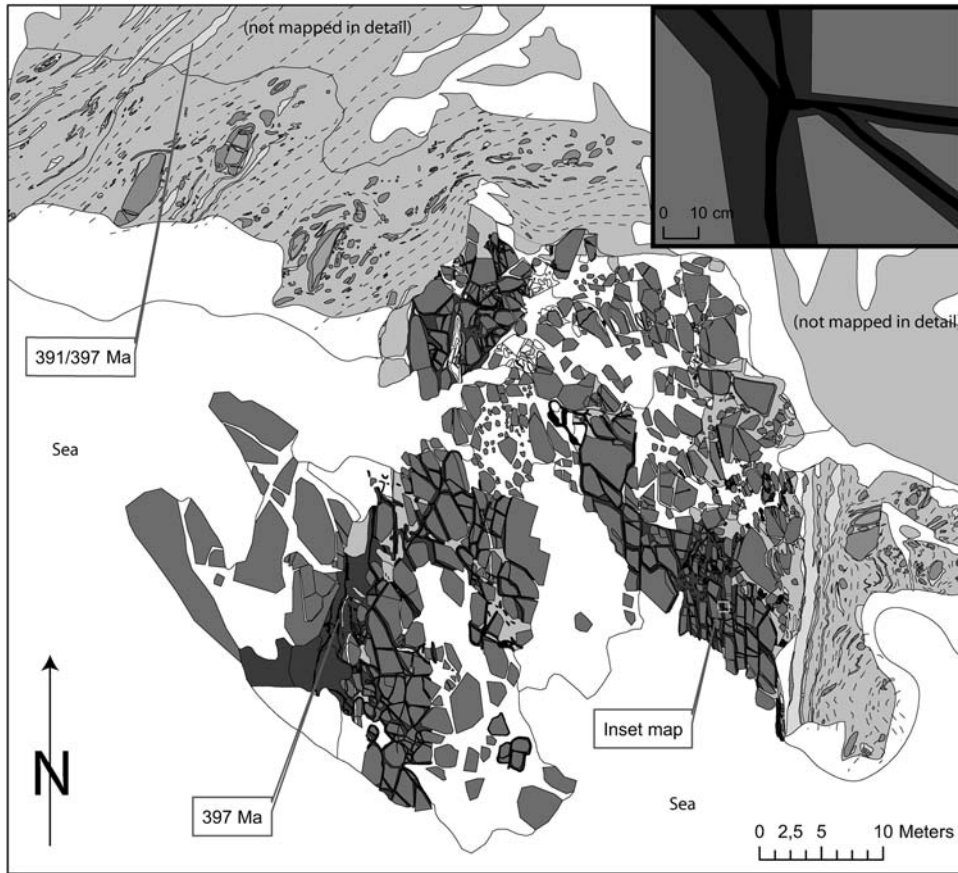


Fig. 3. Geological map of the Svartberget peridotite and surrounding felsic gneiss showing only the major zones of the veins in the conjugate fractures. In the peridotite: grey colours = peridotite; dark grey = grt-phl-websterite; black = garnetite. In surrounding area: light grey = migmatite; medium grey = amphibolitic migmatitic felsic gneiss; grey = eclogite; dark grey = amphibolite. Inset shows a detail of the relation of peridotite with crosscutting veins in the fractures. Ages point to location of zircon samples.

metamorphic growth of zircon in the garnetite at 397 ± 1.2 Ma, either coinciding or predating an initial phase of leucosomes formation (397.4 ± 1.1 or 391.0 ± 1.0), formation or equilibration of garnet and pyroxene in peridotites and crystallization of pegmatite cores, rutile and monazite at 393–388 Ma, and late stages of activity at around 380 Ma.

2.3. Melt infiltration and metasomatism

Field relations suggest that metasomatic reactions took place along the fractures with the peridotite. Whole-rock XRF measurements were performed on the various altered peridotite blocks and the crosscutting websterites. The whole-rock samples of altered peridotite blocks and individual zones in the fractures were compared to the least altered peridotite for mass balance. Mass-balance calculations show a gain in Si, Al, Na, K, Rb, Ba, Sr, Y and Zr and loss of Fe, Mg, Ca, Sc, Zn, V, Cr, Cu and Ni in websterites with respect to most pristine wall-rock samples of the peridotite, indicating metasomatism of the Svartberget peridotite.

Sr isotopes in grt, cpx and whole rock of the veins and peridotite have a crustal signature matching the Sr isotopes in the gneiss, indicating that melts from the gneiss infiltrated the peridotite. Measured $^{87}\text{Sr}/^{86}\text{Sr}$ ratios were

calculated back to 400 Ma, the time of the Caledonian UHP event. Initial $^{87}\text{Sr}/^{86}\text{Sr}$ values start from elevated values about 0.723 in most pristine peridotite samples and show an increasing trend up to ~ 0.743 in most altered samples in veins. All initials are about ten times higher than would be expected from a mafic-ultramafic rock. Whole-rock samples from leucosomes and gneiss yield Sr initial values around 0.75 and are the most likely source for the crustal signature of Sr in the peridotite.

The polyphase solid inclusions have been interpreted as precipitates from a supercritical C–O–H fluid and such inclusions have been observed in other places in association with microdiamond (Stöckhert *et al.*, 2001; Carswell & Van Roermund, 2005). These supercritical fluids are probably more complex than just C–O–H because the assemblages in the polyphase inclusions consist of a wide variety of minerals (Vrijmoed *et al.*, 2006, 2008). The fact that these polyphase solid inclusion assemblages are distributed randomly in the garnet crystals strongly suggests that the fluids were trapped when garnet formed. Sm–Nd cooling ages obtained from grt–cpx mineral separates show that garnet formed during the Caledonian event and suggest that the complex supercritical fluids infiltrated the fractures during the Caledonian. The incompatible elements that were

transported into the polyphase inclusions indicate a crustal origin of the fluids/melts. The most likely source of these fluids/melts including carbon to form diamond is the host-rock gneiss of the peridotite, which is in agreement with the bulk-rock chemistry and Sr isotope data.

3. Conceptual model

The essence of our conceptual model is that a volume-increasing reaction (partial melting of the gneiss) takes place in a space with a confined volume held by a container (the lithosphere). The result of such a reaction is an increase in pressure. The pressure is released as soon as the space is not confined anymore (*i.e.*, when the container breaks). In the following section we will explain this for a general case and apply it to the case of the Svartberget peridotite.

3.1. Melting in confined space

Commonly, when two continents collide, a thickened crust develops with a mountain belt on top and a root below to maintain isostasy. During this process crustal rocks are being buried as the crust thickens. The lower crust consists of different materials, both ortho- and paragneiss. When rocks become metamorphosed during the burial, partial melting in pelitic gneiss is likely to occur above a certain temperature. It is however not likely that the whole lithosphere starts melting. Thus a situation develops in which partial melting starts in certain volumes of rock surrounded by non-molten rocks. This situation is illustrated in Fig. 4. A similar situation develops in a subduction scenario as shown by Gerya *et al.* (2008) in which melting of subducted sediments takes place in a large area between 30–80 km depth at 1.5 GPa and 600–700 °C. This melting area is surrounded by non-molten rocks of the rigid walls of the subduction channel and non-molten rocks above and below (see Fig. 4 in Gerya *et al.*, 2008).

The partially molten area is surrounded by solid rocks. Partially molten gneiss will have a lower density than solid rocks and will need to expand as a result of the melting (Fig. 4b). However the rocks that are not melting will not expand and a space problem develops. Therefore the melting region cannot expand and instead it will raise the pressure (Fig. 4c). Although the surrounding rocks of the lower crust might be relatively weak, the upper crust and upper mantle confine the space and act as a container. When lithosphere-scale fractures develop, for example extensional faults, this container breaks and pressure will be released (Fig. 4d).

Melting in a confined space can be understood from a simple binary solid-solution system which can be approximated by ideal solutions. For more complex multicomponent systems such as pelitic gneiss, the thermodynamics is more complicated but the principle is the same. In Fig. 5 a P - T diagram of volume and melt percentage is shown for the forsterite-fayalite binary system.

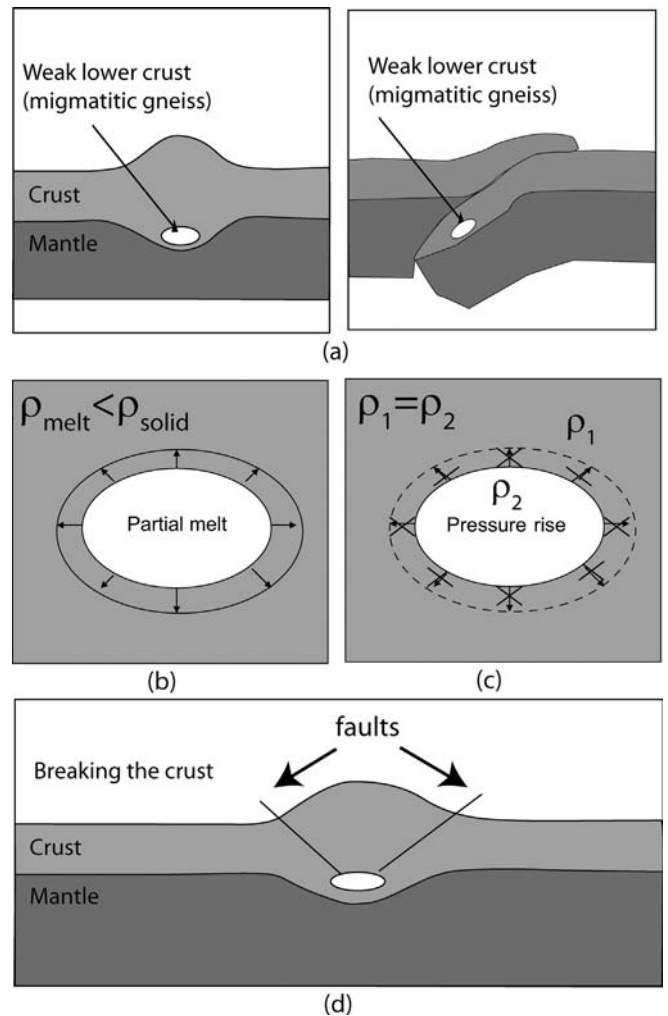


Fig. 4. Figures showing the conceptual model discussed in this study. (a) Initial situation in which rocks from the lower crust are buried due to continental collision. It is reasonable to assume that not the whole crust that is heated by burial will melt. So we consider that certain areas start producing partial melt, which could happen both in a classical continental thickening scenario or a continental subduction scenario. (b) During this melting the rocks will have to expand because the density of melt will be lower than that of solid. (c) Because surrounding rocks are not melting, the melting area is now confined to a certain volume, therefore the rocks will not be able to melt as much as they would in unconfined space. As a result the pressure in the melting area has to rise. (d) The pressure will rise up to a point where the rocks that formed the container break due to formation of large-scale faults. When the pressure is released, extensive decompression melting can take place.

Consider what happens when temperature increases up to a point where melting starts. First volume will expand gently due to thermal expansion, until the rocks reach the solidus. At this point volume increases more rapidly and if the volume is confined the rock will stay on equal volume lines (isochores). When temperature keeps rising the rock will follow a path on an isochore increasing in T and inevitably also in P . From the P - T diagram where melt percentage is contoured, it can be seen that isopleths of melt directly follow isochores, which means that melt

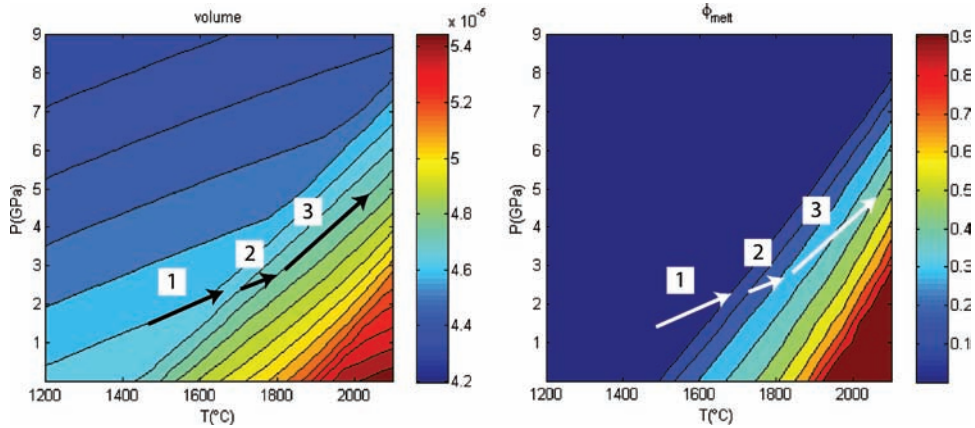


Fig. 5. Concept of melting in a confined space for a simple binary ideal system as an example. (a) P - T diagram showing the volume of a system consisting of pure olivine calculated from the thermodynamic database of Holland & Powell (1998), assuming ideal mixing for both solid and liquid. Below a certain temperature (depending on P) the diagram shows gently dipping slopes of equal volume (isochores) in P - T space. This represents the increase in volume due to thermal expansion and the decrease in volume due to increase in P . Above this certain temperature isochores become much steeper, which means that with increasing temperature a much stronger increase in volume takes place. This is the result of melting as can be seen in a plot of melt percentage in (b). The arrows indicate a hypothetical P - T path. First dry rocks that approach the solidus (arrow 1). Above the solidus the system starts to produce some melt (step 2) but now imagine that the volume is constrained. Then it has to follow lines of equal volume (step 3) and, if temperature keeps increasing with the same amount, the pressure suddenly increases much more than before. (b) The same P - T path is drawn on top of a diagram showing the fraction of melt. It can be seen that melting is greatly reduced while the rocks are constrained. Because rocks are never perfectly incompressible it is still possible to accommodate some melting.

percentage will not increase during such an isochoric melting process.

3.2. Application to Svartberget

The available whole-rock, geochronological and isotope data from the Svartberget peridotite body suggest that the rocks were in a situation where surrounding gneissic rocks started melting during the Caledonian orogeny. Therefore the concept explained in the previous section can be applied to the rocks at Svartberget.

We start the conceptual model at the point where rocks are buried to 70 km, as can be constructed from structural data in the southern part of the WGR (Fig. 1). The strong peridotite is included in the weak gneiss of the lower crust which is itself sandwiched between the upper crust and mantle (Fig. 6a).

The Svartberget rocks are situated in the structurally lowest part in the north of the WGR and are likely to have been buried deeper, perhaps as deep as 90 km. During this burial the rocks will cross the melting boundary from 700 to 800 °C (Hermann & Spandler, 2008) and melting in the confined space will rise the pressure up to 5.5 GPa (Fig. 6b). The peridotite is strong and holds its original low pressures.

The melt that is formed in the gneiss will be present between the mineral grains at a very high pressure and exert a pressure on the peridotite (Fig. 6c). Figure 7 is an enlargement of the situation on the boundary between gneiss and peridotite. A sketch of the state of stress of the peridotite is visualised by the Mohr circle in Fig. 7a.

The pressure of the melt or fluid (P_f) will lower the strength of the peridotite, resulting in a shift of the Mohr

circle to the left where it meets the brittle-failure criterion. The fracture set that develops is a conjugate set having 60° angles (Fig. 6d). These fractures provide a pathway for the supercritical fluids to infiltrate the peridotite and metasomatise the rock to form a metasomatic column consisting mainly of phl-grt-websterites and garnetite (Fig. 6e). Because these supercritical fluids are physically connected to the gneiss and have the high pressures (5.5 GPa), diamond-grade conditions will be recorded in the websterites. The blocks of peridotite that are not broken will maintain their original pressure due to their strength.

Finally when for example extensional structures form in the orogen the container will break. When this happens the pressures are released and decompression melting takes place (Fig. 6f). Now that the gneiss is not constrained anymore to a certain volume, it will start to deform ductily more heavily and, together with all the fluids released from dehydration reactions, retrogression in the gneiss is quick and destroys any record of UHP. The release of such a highly pressurised unit of rocks is a potentially good exhumation mechanism, very similar to but perhaps less catastrophic than volcanic eruptions. A summary of the conceptual model for the Svartberget peridotite is given in Fig. 8.

4. Numerical test

To understand how a system will behave mechanically in a setting as described above we conducted numerical tests using FEM. We found that pressure variations are

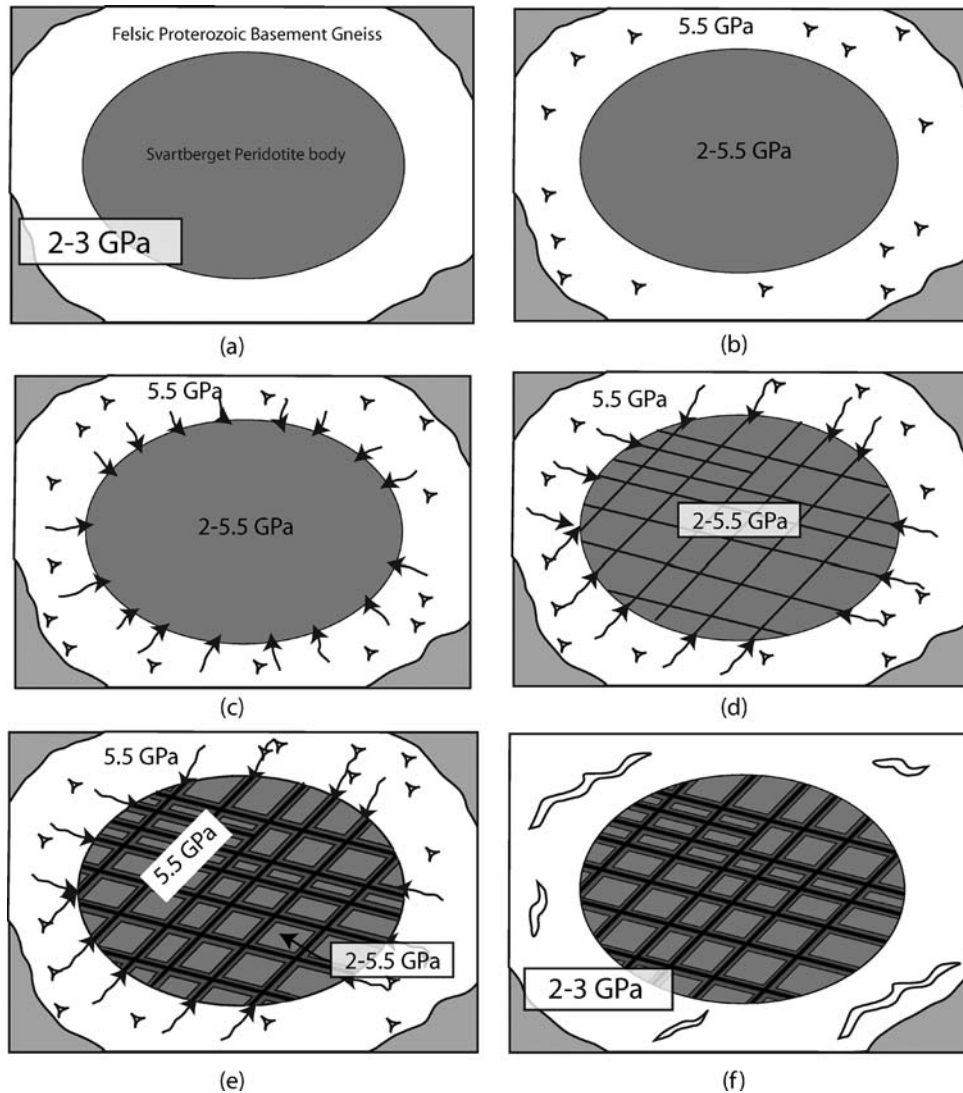


Fig. 6. Conceptual model accounting for observed features in Svartberget. (a) Initial stage where the Svartberget body is enclosed in basement gneiss of the WGR somewhere in the lower crust. (b) During burial and heating, rocks surrounding the peridotite start to melt but surrounding non-molten rocks confine the space and pressure builds up (c). The small amount of interstitial melt that accumulates between grains adjacent to the peridotite lowers the yield strength of the peridotite (Fig. 7). (d) The lowering of the yield strength causes the rock to reach the brittle-fracture criterion and conjugate brittle shear fractures develop. (e) As soon as fractures propagate into the peridotite, melt (or supercritical fluid) that has the same pressure (5.5 GPa) as the surrounding gneiss can flow in. This supercritical fluid is now highly reactive and metasomatism takes place at UHP conditions along the fractures capturing micro-inclusions of diamond while growing. (f) Finally the lithosphere holding the overpressured gneiss constrained breaks due to formation of large-scale fractures in the crust and decompression melting starts and, now that the gneiss is not constrained to a certain volume, it can flow ductily and it is highly unlikely that any UHP mineral survived in such a deforming fluid-rich environment.

expected in the case when gneiss starts melting while it is enclosed in a ten to hundred times stronger container and has a peridotite enclave with the same strength as the container. Intuitively it might be expected that a peridotite enclave enclosed in pressurised confined melting gneiss would experience the same pressures as the gneiss. However the results of our mechanical modelling show that in this case pressures in the expanding gneiss are highest, while pressures in the peridotite are much lower than in the gneiss but still higher than in the containing lithosphere. Our results are discussed in more detail in the rest of this section.

4.1. Methods

We use a 2D FEM code written in Matlab with triangular elements on a mesh that is generated using the mesh generator “Triangle” (Shewchuk, 2005). The system of equations that we solve consists of the stress balance equations and a rheology law, either completely elastic (Hook’s law) or viscous (Newton’s law) including thermal strain that results from melting in a confined space. We use a setup with three nested cylinders that can be given different material properties. The outermost cylinder is our analogue for the lithosphere or the container, the middle cylinder

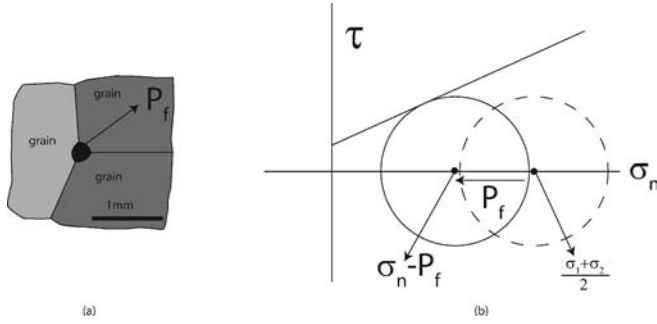


Fig. 7. This figure illustrates how fracturing initiates at the contact of gneiss and peridotite. (a) A melt pocket (black) situated between grains of peridotite and gneiss with a high pressure lowers in that point the yield strength of the material. (b) This figure illustrates how the state of stress at the location of melt shifts and hits the brittle-failure envelope. As soon as this happens a fracture propagates into the peridotite and melt can percolate in, lowering the yield strength again and the fracture can propagate further. This is likely to happen along the whole boundary between gneiss and peridotite. (P_f = fluid (melt) pressure; σ_n = normal stress; σ_1 = principal stress 1; σ_2 = principal stress 2; τ = shear stress).

simulates the migmatitic gneiss and the innermost cylinder is analogue to the peridotite. The outermost boundary of the outermost cylinder is fixed in one point. The middle cylinder is expanding due to a rise in temperature. The shape of the peridotite can be varied. Results of systematic variations of the parameters are documented below.

4.2. Results

Results are shown in Fig. 9 and described below. The results are presented as colour coded 2D plots zoomed in on the area of interest (the boundaries of the outermost cylinder are far away). The colours correspond to values of a dimensionless pressure (\tilde{P}) for a Poisson's ratio of 1/3:

$$\tilde{P} = \frac{\beta \Delta P}{\alpha \Delta T} \quad (1)$$

Where α = thermal expansion coefficient, β = compressibility, and the ΔP and ΔT are the increments of pressure and temperature during the process. Poisson's ratios in rocks at depth are lower than the 1/3 we have used here (Gercek, 2007) and vary between different rock types, however it does not influence our results significantly. The choice is convenient because the conversion of Young's modulus (E) converts nicely into compressibility to arrive at the expression in Equation (1). If we rearrange this equation, we get an expression similar to the relation between pressure and temperature in a confined space given in Turcotte & Schubert (2002) (p. 172, Eq. 4–180):

$$\Delta P = \tilde{P} \frac{\alpha}{\beta} \Delta T \quad (2)$$

The exception is that the equation given here above includes the dimensionless pressure that we calculated. Our calculations can also be used for purely viscous

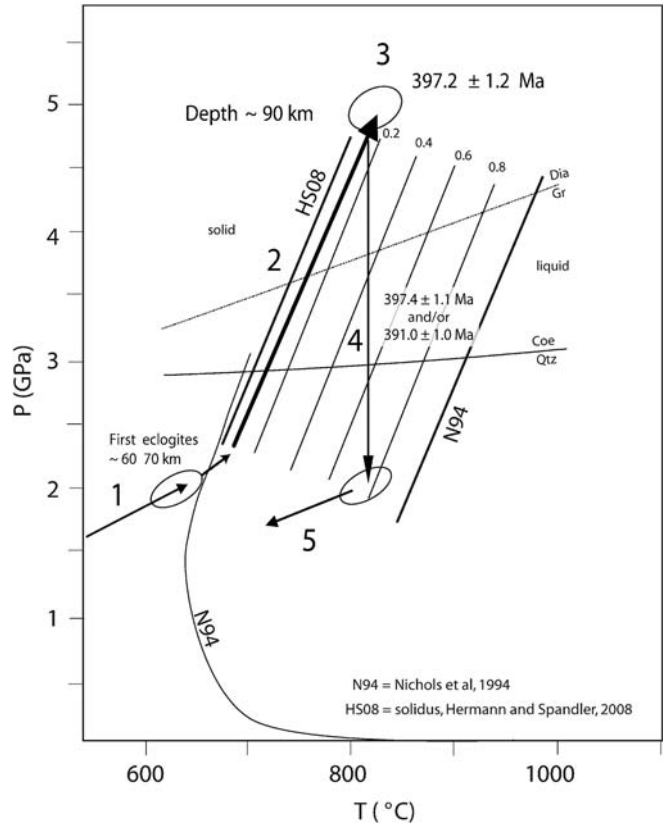


Fig. 8. Summary of the conceptual model displayed in P - T space. The P - T trajectory is shown with arrows 1–5. In the first stage of collision rocks become buried and, in the south of the WGR, reached a depth of 60–70 km in agreement with structural field reconstructions. In the north of the WGR rocks are positioned structurally below this and reached a depth of 90 km at the most. However, during this path the gneiss surrounding the Svartberget peridotite started melting in a confined space and followed approximately the melt isopleths. During this process the pressures increased up to 5.5 GPa where fractures in the peridotite developed and metasomatism took place, including the precipitation of diamond. Then the confined space was broken and pressure was released (arrow 4) resulting in extensive melting and new zircon growth in leucosomes. Finally the rocks were exhumed at 5 along the observed structures in the field. The model is inspired by fieldwork in East Greenland, and accompanying force and energy balanced models (Hartz *et al.*, 2007). (Dia-Gr and Coe-Qtz equilibrium lines calculated from Holland & Powell, 1998; isopleths of melt indicated by near vertical thin black lines taken from Hermann & Spandler, 2008; HS08 = solidus taken from Hermann & Spandler, 2008; N94 = liquidus taken from Nichols *et al.*, 1994; sol = solid; liq = liquid; ages are single zircon U-Pb data for garnetite at 3 and leucosome at 4).

rocks under the condition that the total strain during a given increase in temperature is the same. This is the case for our model, because the strain is a result of the melting reaction and is therefore the same in both viscous and elastic cases. Then the equation can be rewritten as:

$$\Delta P = \tilde{P} \eta \alpha \frac{\Delta T}{\Delta t} \quad (3)$$

Known values from literature can be substituted for α (thermal expansion coefficient) and η (viscosity) over a

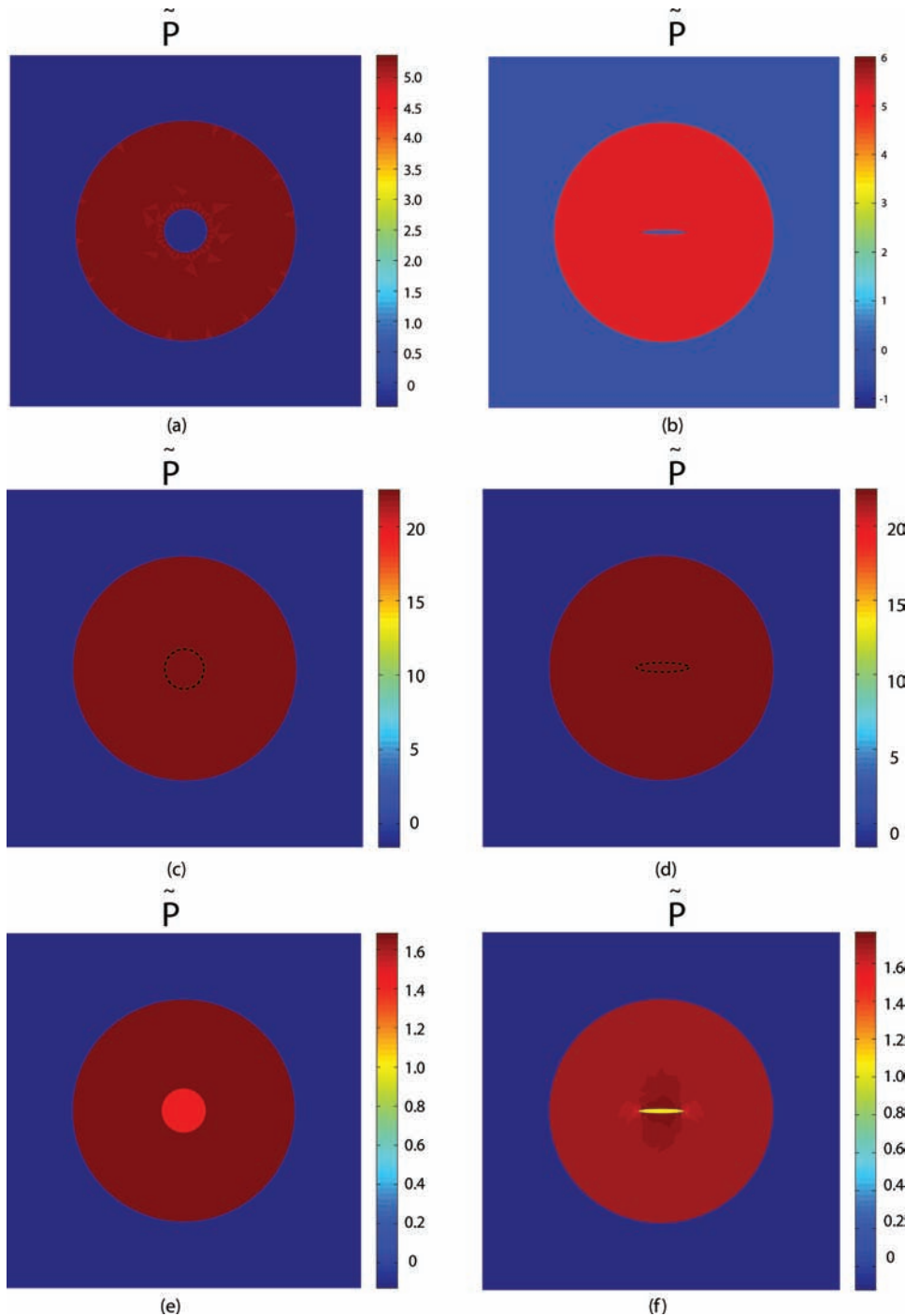


Fig. 9. Results of the 2D FEM calculations plotted for dimensionless pressure. (a) In this case we calculated the pressures with equal strength of migmatitic gneiss, peridotite and non-molten containing lithosphere. The figure shows that the partially molten gneiss has a high overpressure while the peridotite and containing lithosphere have the same pressure and are hardly affected by the melting in the gneiss. (b) The same parameters as in (a) but only with a different shape of peridotite. It can be seen that there is no significant effect on the pressure distribution (N.B. colours are different but values are the same). (c) Result for the case that the migmatitic gneiss is 10^5 times weaker than the peridotite and surrounding lithosphere. It can be seen that pressures are very high in the migmatitic gneiss and equally high in the peridotite and low in the surrounding lithosphere. (d) The same result as in (c) is obtained for different aspect ratios. (e) These results show the case where the migmatitic gneiss is ten times weaker than the lithosphere and peridotite. Here highest pressures are obtained in the migmatitic gneiss, lowest pressures in the surrounding lithosphere and intermediate pressures (but higher than the surrounding lithosphere) in the peridotite. (f) The same parameters are applied for this figure, but a different aspect ratio which results in higher pressure in the peridotite and slightly heterogeneous pressure distribution in the migmatitic gneiss.

given temperature interval ΔT during a given period in time Δt to obtain the corresponding pressure increase ΔP . In the purely elastic case we can use Equation (2). In that case ΔP will represent the total pressure increase starting from zero pressure.

When the strength of the container, gneiss and peridotite are all equal, overpressure builds up in the gneiss, and the container and peridotite have the same pressure. Fig. 9a, b shows the results of the calculations in the case of equal strengths of all three units for a spherically and elliptically shaped peridotite respectively. This situation produces large overpressures in the gneiss but the pressures in the peridotite are the same as in the container. However, felsic gneiss with hydrous minerals in the lower crust is likely to be much weaker than the upper crust and mantle or ultramafic rocks such as peridotite.

If the gneiss is five orders of magnitude weaker than the peridotite and container, large overpressures are obtained in the gneiss and equally high overpressures are obtained for any shape of peridotite. The results are shown in Fig. 9c, d for different geometries. This case is more realistic in the sense that now the gneiss is weaker than the container and peridotite. But it does not explain how pressures in the peridotite can be lower than in the fractures that were inferred to have the same pressure as the gneiss.

If the gneiss is ten to hundred times weaker than the peridotite and container, the pressure in the gneiss is highest, while the pressure of the peridotite is higher than the container. This situation is probably the most realistic of the three presented here because the gneiss is not likely to be five orders of magnitude weaker than the other rocks. In this case we can explain the pressure variations that we observe in the field.

5. Discussion

Whether the overpressure resulting from the melting in a confined space is a plausible mechanism to account for the UHP in the Svartberget peridotite depends on how much pressure the container can hold before it breaks and the magnitude of the pressure that can be obtained from the melting reaction. Further questions that will be addressed here are what rocks in the field may represent the container, if the melt reaction would increase the volume and whether the Svartberget rocks are a unique case.

With the modelling results presented in Fig. 9 it is now possible to estimate the pressures that will be generated using estimated values for the individual parameters of the dimensionless pressure. A typical value of β for rocks is 10^{-11} (Turcotte & Schubert, 2002). The thermal expansion coefficient can be obtained from the solidus and liquidus in P - T space, for example from the diagram in Hermann & Spandler (2008) and Fig. 8. Reading the values from the diagram combined with the densities of

the solid and liquid, we can use the expression below to calculate α :

$$\alpha = \frac{1}{V_{\text{ref}}} \frac{(V_{\text{new}} - V_{\text{ref}})}{(V_{\text{new}} - V_{\text{ref}})} \quad (4)$$

We can obtain volumes per unit mass from the densities ($V = 1/\rho$). As an approximation we use density of granite and granite melt, 2650 kg/m^3 (Turcotte & Schubert, 2002) and 2290 kg/m^3 (Bass, 1995) to calculate V_{ref} and V_{new} , respectively. Although the densities change with pressure and temperature, this is not a significant change and serves as a good approximation. Reading from the diagram the temperature T_{ref} at the solidus and T_{new} at the liquidus we obtain, using Equation (4), $\alpha \sim 6.79 \cdot 10^{-4} \text{ K}^{-1}$.

The pressure would increase by 12.2 GPa during an increase in temperature of $100 \text{ }^\circ\text{C}$ in the purely elastic case (using Equation 2). In the purely viscous case we can, under certain assumptions, replace the compressibility by viscosity/time and use Equation (3). It can be easily seen that the longer it takes to melt to a certain degree, the smaller the resulting overpressure is. Using effective viscosities of 10^{22} taken from literature as a first approximation (Kaus *et al.*, 2008), the overpressure while melting to 50 % over a time span of 10,000 years is 3.9 GPa and it is about 1.95 GPa when melting reaches 50 % within 50,000 years.

The arguments used here for the existence of a container that confines the space in which melting takes place are straightforward. It is unrealistic to have the whole lithosphere molten, consequently if rocks become subject to partial melting they will always be surrounded by non-molten rocks. If the melting reaction comes with an increase in volume then the rocks will expand while the non-molten rocks will not and will act as a container. In order to sustain pressure difference of 1–2 GPa the container must have sufficient strength, *i.e.* to be able to hold differential stresses of similar magnitude. Laboratory experiments confirm that rocks of all major compositions may sustain differential stresses up to 1–1.5 GPa (*e.g.*, Renshaw & Schulson, 2007). However, it is commonly believed that the differential stress level is low (significantly less than a 0.1 GPa) in the Earth's mantle and lithosphere at much larger time and length scales. This can be due to strength of the rocks lower than extrapolated from laboratory measurements, or lack of the mechanism able to generate high stresses. Seismologists report earthquakes stress drops in subduction settings up to 0.25 GPa (Kanamori, 1994), which represents the lower bound of the maximum stress (Scholz, 2004). Geological records suggest 0.5–0.6 GPa stress drop (Trepmann & Stockhert, 2003; Andersen *et al.*, 2008) indicating that the maximum stress must have been higher and agrees well with estimations of the stress drop presented in John *et al.* (2009). Indeed, recent field data from Andersen *et al.* (2008) on pseudotachylytes in Corsica indicate both that upper-mantle lithospheric rocks in fact could sustain high differential stresses (Andersen *et al.*, 2008) and that high differential stresses were generated. High loading rates may be related to the 100 year earthquake cycles or any other high-

frequency dynamics of the subduction zone factory (Kelemen & Hirth, 2007). But even on the slow rates of deformation ($\sim 10^{-14} \text{ s}^{-1}$) numerical experiments show need for the maximum stress of 1–1.5 GPa to initiate an unstable earthquake-like deformation mode (Kelemen & Hirth, 2007). Trepmann & Stöckhert (2001) interpreted microstructural evidence in an eclogite-facies metagranite to be produced by differential stresses from 0.5 up to 1.0–2.0 GPa. To conclude, high stress levels up to 1 GPa may be much more often reachable in natural settings than previously anticipated.

Even if the non-molten rocks immediately surrounding the partially molten gneiss were too weak at 800 °C, they still form part of the lithosphere and must have had a strong crust on top and an upper mantle below. The alternative is that we had a crustal asthenosphere and crustal isostasy in which everything in the lower crust is in lithostatic equilibrium. Since field gravity measurements in 1851, it has been clear that mountains have roots and the first level of isostasy is in the mantle. Therefore it means that lithospheric rocks are strong enough to hold undulations of both topography and Moho (the upper and low parts of the container) for considerable geological time. According to the classic “rheology independent Jeffreys argument” (Kanamori, 1980), the differential stress averaged over 100 km thickness of the lithosphere must be at the level of 0.1 GPa to support the mountains and their roots. John *et al.* (2009) reasoned that, if concentrated to a 10 km stress guide within an otherwise weak plate boundary or to a similar-size strong (cold) block of rock acting as a stress concentrator, the stress level may reach the level of 1.0 GPa needed for failure even in their most simple simulations ($0.1 \text{ GPa} \times 100 \text{ km}/10 \text{ km} = 1 \text{ GPa}$). A similar argument can be suggested in 3D. For example, a strong exhuming block of lithosphere of 50 km lateral and cross-sectional extent within a 500 km long, very weak ($<0.1 \text{ GPa}$) plate boundary having high mountains (*e.g.*, Andes) would concentrate 2 GPa stresses ($0.1 \text{ GPa} \times 500/50 \times 100 \text{ km}/50 \text{ km} = 2 \text{ GPa}$). To conclude, an ability of rocks to hold differential stress levels up to 2 GPa is required to sustain topography of mountains and their roots, especially if a significant part of the lithosphere is weakened by melting or any other mechanism along the weak plate boundary.

Large pressure variations can be sustained in inclusions in mechanically strong minerals such as garnet (Chopin, 1984; van der Molen & van Roermund, 1986; Zhang, 1998; Ye *et al.*, 2001; Chopin, 2003; Perrillat *et al.*, 2003; Chopin *et al.*, 2008; O’Brien & Ziemann, 2008), but may be suspected to drop dramatically in polycrystalline rocks. However, laboratory measurements on the rheology of eclogite show that the strength of such rocks is a simple mechanical mixture of the pure end-members garnetite and weaker omphacite rather than a dramatically weaker rock type (Jin *et al.*, 2001). If garnet can sustain 1–2 GPa overpressure and the mixture of garnet and cpx rheologically is not orders of magnitude weaker, it seems plausible that pressure variations can be sustained also on the larger scale.

From a field-geology perspective it might be questioned what rocks represent the container (referred to here as containing lithosphere occasionally). In the WGR there are many differences in amount of migmatization of the gneisses and the Svartberget peridotite is located in an area that shows some of the most migmatized rocks, equivalent to local units such as the Ulla Gneiss (Terry & Robinson, 2003). In contrast to those rocks, there are low-strain Proterozoic plutonic granitic rocks to the north at Drøga and Hustad (Austrheim *et al.*, 2003) and relatively low strain rapakivi-type augen orthogneiss near Molde to the south of the Svartberget gneisses (Harvey, 1983). These rocks are situated structurally above and below the migmatitic Svartberget gneiss (Ulla gneiss) and could possibly represent the container, which now is broken and will not form a coherent closed seal anymore. It must be noted here though that it is possible that late transverse movement associated with movement along the Møre Trøndelag Fault Zone (MTFZ) (Seranne, 1992) might have offset rock units in this area out of its original context. Possible thrust movement of the rock units is yet unconstrained in this area as it is difficult to identify major tectonic contacts. It is thus still possible that the rocks were approximately in their original context and their relative low grades of migmatization and deformation might indicate their relative strength as a container.

In a subduction setting it is likely that the walls of the container would never be exhumed as they would be represented by the rigid walls of the subduction channel. In this setting UHP rocks within the channel will be exhumed but not the channel itself (see Gerya *et al.*, 2008).

Another immediate question to the concept presented here is whether the melt that forms has a higher or lower density (*i.e.*, whether it is expanding or contracting). Depending on fluid-absent or fluid-present melting conditions, the volume of melt is respectively larger or smaller than volume of the solid (Clemens & Droop, 1998). On the other hand, melt (or fluid) is more compressible than solid, so density crossovers are expected at higher pressures. For the case of the Svartberget conceptual model starting at 2–3 GPa, it is likely to have fluid-absent melting conditions and still far away from the density inversion where melt becomes heavier than solid (Suzuki & Ohtani, 2003). It can also be inferred from the positive slope of the experimentally derived melt isopleths in Fig. 8.

In the conceptual model described above, the fracturing in the Svartberget peridotite is a result of the lowering of the yield strength of the peridotite by pore fluid (melt) pressure. The same might happen on the side of the container and as such the boundaries of the container will be moving at the speed of the propagation of this fracture front. It is likely that it will take longer to break through the whole pile of rocks above and below than to fracture a small peridotite enclave.

We have illustrated the situation in a conceptual way in Fig. 10. In fact the fracturing of the container is likely to occur as illustrated in Fig. 10a and it will fracture strong upper-mantle or lower crustal gabbro/peridotite rocks

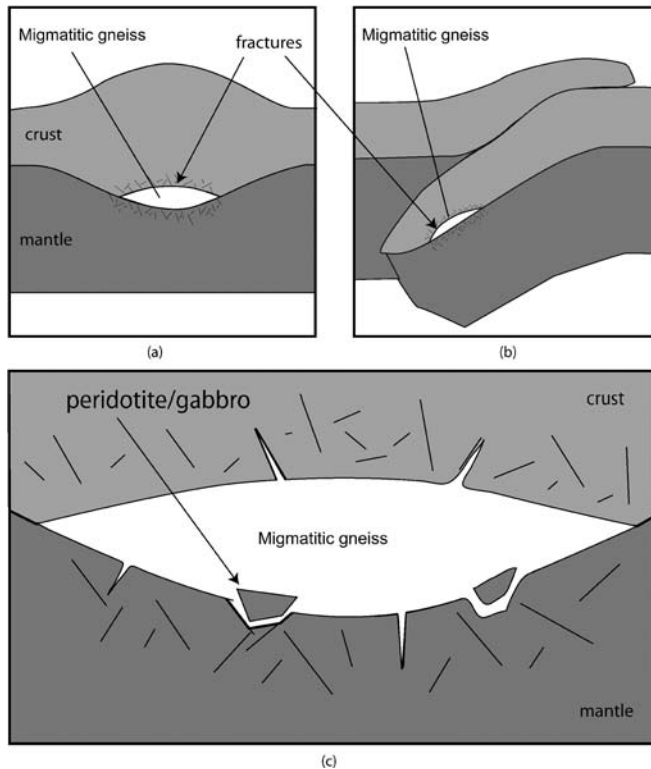


Fig. 10. Conceptual model showing the fracturing around the pressurised partially molten rocks of the lower crust applicable to both (a) a crustal thickening model and (b) a subduction model. (c) Close up of the partially melting lower crust. Due to geometrical effects of the partially molten pressurised rock volume, differential stresses in the surrounding non-molten lithosphere will lead to fracturing. Here it is conceptually shown how the weak partially molten gneisses penetrate into these fractures driven by the pressure gradient from pressurised partially molten rocks to lower pressure non-molten rocks. Locally, migmatitic gneiss may surround the fractured (ultra-) mafic rocks and metasomatise them as observed in the Svartberget peridotite.

below and mid-upper crustal rocks above. This would explain the reason for fracturing of otherwise undeformable peridotite/gabbro at this moderate temperatures and infiltration of partial melts into the fractures of the peridotitic rocks that are positioned below the melts. In a subduction channel this might occur on both the footwall side and the hanging-wall side of the channel.

Although a common consensus exists about the deep origin of the UHPM (Green, 2005) and several conceptual and sophisticated numerical models of deep continental subduction exist (Brueckner & Van Roermund, 2004; Hacker, 2007; Gerya *et al.*, 2008), the problem remains that structures in the field only show the last part of the exhumation from the large depths derived from a lithostatic pressure assumption. The structural geology of the Western Alps has been studied in detail and reconstructions along several profiles through that part of the orogen that is famous for its coesite discovery in the Dora-Maira massif (Chopin, 1984) are often insufficient to explain the exhumation of the coesite-bearing rocks from depths of 100 km (Platt, 1986; Wheeler, 1991; Avigad *et al.*, 2003; Ford *et al.*, 2006). Or some reconstructions show that rocks

might have been at greater depth than inferred from their P - T estimates, in other words they did not record the (U)HP and may have escaped through a subduction channel (Michard *et al.*, 2004).

In addition, many UHP rocks are situated in a similar setting as the Svartberget peridotite, where UHP eclogites or peridotites are surrounded by migmatitic gneiss that shows no signs of UHPM. The Alpe Arami garnet-peridotite massif in the central Alps displays UHP mineralogy while the surrounding, kyanite-bearing Lepontine gneisses display evidence of partial melting, but lack mineral relics indicative of UHPM and represents a field of active research (Ernst & Liou, 2008).

If structural reconstructions in UHP areas cannot account for the amount of burial needed to explain lithostatic pressures, or lack of fluids (Austrheim, 1987) and sluggish kinetics did not seem to be the problem, then it might be worth investigating a possible explanation as we propose here for the Svartberget peridotite.

6. Conclusion

From the first-order quantifications presented in this paper we can conclude that melting of gneiss in the weak lower crust can result in significant overpressures that are sustainable on the geological time scale.

Melting of gneiss in confined space where the gneiss is weaker than its container and inclusions provides a mechanism for pressure variations in rocks.

We can therefore conclude that the model of melting gneiss in confined space is a possible mechanism to account for the pressure variations and UHP metamorphism in the Svartberget peridotite.

Acknowledgements: This project was funded by the Norwegian Research Council as part of the funding of Physics of Geological Processes (PGP) for the PhD of J.C. Vrijmoed. We thank all PGP people for extensive discussions, in particular Nina Simon and Timm John. Marcin Dabrowski kindly provided help with the numerical modelling.

References

- Andersen, T.B., Mair, K., Austrheim, H., Podladchikov, Y.Y., Vrijmoed, J.C. (2008): Stress release in exhumed intermediate and deep earthquakes determined from ultramafic pseudotachylite. *Geology*, **36**, 995–998.
- Austrheim, H. (1987): Eclogitization of lower crustal granulites by fluid migration through shear zones. *Earth Planet. Sci. Lett.*, **81**, 221–232.
- Austrheim, H., Corfu, F., Bryhni, I., Andersen, T.B. (2003): The Proterozoic Hustad igneous complex: a low strain enclave with a key to the history of the Western Gneiss Region of Norway. *Precambrian Res.*, **120**, 149–175.

- Avigad, D., Chopin, C., Le Bayon, R. (2003): Thrusting and extension in the southern Dora-Maira ultra-high-pressure massif (Western Alps): view from below the coesite-bearing unit. *J. Geol.*, **111**, 57–70.
- Bass, J.D. (1995): Elasticity of minerals, glasses, and melts. in “Mineral physics and crystallography”, T.J. Ahrens, ed. American Geophysical Union, Washington, DC, 45–63.
- Bea, F., Pereira, M.D., Stroh, A. (1994): Mineral/leucosome trace-element partitioning in a peraluminous migmatite (a laser ablation-ICP-MS study). *Chem. Geol.*, **117**, 291–312.
- Blundy, J., Cashman, K., Humphreys, M. (2006): Magma heating by decompression-driven crystallization beneath andesite volcanoes. *Nature*, **443**, 76–80.
- Brey, G.P. & Köhler, T. (1990): Geothermobarometry in four-phase Lherzolites II. New thermobarometers, and practical assessment of existing thermobarometers. *J. Petrol.*, **31**, 1353–1378.
- Bruceckner, H.K. & van Roermund, H.L.M. (2004): Dunk tectonics: a multiple subduction/duction model for the evolution of the Scandinavian Caledonides. *Tectonics*, **23**, TC2004, doi:10.1029/2003TC001502.
- Carswell, D.A. & van Roermund, H.L.M. (2005): On multi-phase mineral inclusions associated with microdiamond formation in mantle-derived peridotite lens at Bardane on Fjortoft, west Norway. *Eur. J. Mineral.*, **17**, 31–42.
- Chopin, C. (1984): Coesite and pure pyrope in high-grade blueschists of the Western Alps: a first record and some consequences. *Contrib. Mineral. Petrol.*, **86**, 107–118.
- (2003): Ultrahigh-pressure metamorphism: tracing continental crust into the mantle. *Earth Planet. Sci. Lett.*, **212**, 1–14.
- Chopin, C., Beyssac, O., Bernard, S., Malavieille, J. (2008): Aragonite–grossular intergrowths in eclogite-facies marble, Alpine Corsica. *Eur. J. Mineral.*, **20**, 857–865.
- Clemens, J.D. & Droop, G.T.R. (1998): Fluids, *P-T* paths and the fates of anatectic melts in the Earth’s crust. *Lithos*, **44**, 21–36.
- Dabrowski, M., Podladchikov, Y.Y., Hartz, E.H. (2008): Migmatization induced overpressure, East Greenland case study. *Geophys. Res. Abstr.*, **10**, EGU2008-A-11303.
- Ernst, W.G. & Liou, J.G. (2008): High- and ultrahigh-pressure metamorphism: past results and future prospects. *Am. Mineral.*, **93**, 1771–1786.
- Ford, M., Duchene, S., Gasquet, D., Vanderhaeghe, O. (2006): Two-phase orogenic convergence in the external and internal SW Alps. *J. Geol. Soc. London*, **163**, 815–826.
- Gercek, H. (2007): Poisson’s ratio values for rocks. *Int. J. Rock Mech. Min.*, **44**, 1–13.
- Gerya, T.V., Stockhert, B., Perchuk, A.L. (2002): Exhumation of high-pressure metamorphic rocks in a subduction channel: a numerical simulation. *Tectonics*, **21**, 1056, doi:10.1029/2002TC001406.
- Gerya, T.V., Perchuk, L.L., Burg, J.P. (2008): Transient hot channels: perpetrating and regurgitating ultrahigh-pressure, high-temperature crust-mantle associations in collision belts. *Lithos*, **103**, 236–256.
- Gillet, Ph., Ingrin, J., Chopin, C. (1984): Coesite in subducted continental crust: *P-T* history deduced from an elastic model. *Earth Planet. Sci. Lett.*, **70**, 426–436.
- Green, H.W. (2005): Psychology of a changing paradigm: 40+ years of high-pressure metamorphism. *Int. Geol. Rev.*, **47**, 439–456.
- Hacker, B.R. (2007): Ascent of the ultrahigh-pressure Western Gneiss Region, Norway. *Geol. Soc. Am. Spec. Pap.*, **419**, 171–184, doi:10.1130/2006.2419(09).
- Hartz, E.H., Podladchikov, Y.Y., Dabrowski, M. (2007): Tectonic and reaction overpressures: theoretical models and natural examples. *Geophys. Res. Abstr.*, **9**, EGU2007-A-10430.
- Harvey, M.A. (1983): A geochemical and Rb-Sr study of the Proterozoic augen orthogneisses on the Molde peninsula, west Norway. *Lithos*, **16**, 325–338.
- Hermann, J. & Spandler, C.J. (2008): Sediment melts at sub-arc depths: an experimental study. *J. Petrol.*, **49**, 717–740.
- Holland, T.J.B. & Powell, R. (1998): An internally consistent thermodynamic data set for phases of petrological interest. *J. metamorphic Geol.*, **16**, 309–343.
- Jin, Z.M., Zhang, J., Green, H.W., Jin, S. (2001): Eclogite rheology: implications for subducted lithosphere. *Geology*, **29**, 667–670.
- John, T., Medvedev, S., Rüpke, L.H., Andersen, T.B., Podladchikov, Y.Y., Austrheim, H. (2009): Self-localizing thermal runaway as a mechanism for intermediate deep focus earthquakes. *Nat. Geosci.*, **2**, 137–140.
- Kanamori, H. (1980): The state of stress in the Earth’s lithosphere (Course LXXVIII). in “Physics of the earth’s interior: Varenna on Lake Como, Villa Monastero, 23rd July–4th August, 1979”, A.M. Dziewonski, E. Boschi, eds. North Holland, Amsterdam, 531–554.
- Kanamori, H. (1994): Mechanics of Earthquakes. *Ann. Rev. Earth Planet. Sci.*, **22**, 207–237.
- Kaus, B.J.P., Steedman, C., Becker, T.W. (2008): From passive continental margin to mountain belt: insights from analytical and numerical models and application to Taiwan. *Phys. Earth Planet. Int.*, **171**, 235–251.
- Kelemen, P.B. & Hirth, G. (2007): A periodic shear-heating mechanism for intermediate-depth earthquakes in the mantle. *Nature*, **446**, 787–790.
- Labrousse, L., Jolivet, L., Andersen, T.B., Agard, P., Maluski, H., Schärer, U. (2004): Pressure-temperature-time-deformation history of the exhumation of ultra-high-pressure rocks in the Western Gneiss Region, Norway. *Geol. Soc. Am. Spec. Pap.*, **380**, 155–183.
- Michard, A., Avigad, D., Goffe, B., Chopin, C. (2004): The high-pressure metamorphic front of the south Western Alps (Ubaye-Maira transect, France, Italy). *Schweiz. Mineral. Petrogr. Mitt.*, **84**, 215–235.
- Nichols, G.T., Wyllie, P.J., Stern, C.R. (1994): Subduction zone-melting of pelagic sediments constrained by melting experiments. *Nature*, **371**, 785–788.
- O’Brien, P.J. & Ziemann, M.A. (2008): Preservation of coesite in exhumed eclogite: insights from Raman mapping. *Eur. J. Mineral.*, **20**, 827–834.
- Perrillat, J.P., Daniel, I., Lardeaux, J.M., Cardon, H. (2003): Kinetics of the coesite-quartz transition: application to the exhumation of ultrahigh-pressure rocks. *J. Petrol.*, **44**, 773–788.
- Platt, J.P. (1986): Dynamics of orogenic wedges and the uplift of high-pressure metamorphic rocks. *Geol. Soc. Am. Bull.*, **97**, 1037–1053.
- Renshaw, C.E. & Schulson, E.M. (2007): Limits on rock strength under high confinement. *Earth Planet. Sci. Lett.*, **258**, 307–314.
- Root, D.B., Hacker, B.R., Gans, P.B., Ducea, M.N., Eide, E.A., Mosenfelder, J.L. (2005): Discrete ultrahigh-pressure domains in the Western Gneiss Region, Norway: implications for formation and exhumation. *J. metamorphic Geol.*, **23**, 45–61.
- Scholz, C.H. (2004): The mechanics of earthquakes and faulting. 2nd ed. Cambridge University Press, Cambridge, 496 p.

- Seranne, M. (1992): Late Paleozoic kinematics of the Møre-Trøndelag Fault Zone and adjacent areas, central Norway. *Norsk Geol. Tidsskr.*, **72**, 141–158.
- Shewchuk, J.R. (2005): Triangle 1.6. in “<http://www.cs.cmu.edu/~quake/triangle.html>”, Internet, Berkeley. Smith, D.C. (1984): Coesite in clinopyroxene in the Caledonides and its implications for geodynamics. *Nature*, **310**, 641–644.
- Sobolev, N.V., Shatsky, V.S., Vavilov, M.A., Goryainov, S.V. (1994): Zircon of high-pressure metamorphic rocks from folded regions as a unique container of inclusions of diamond, coesite, and coexisting minerals. *Doklady Akad. Nauk*, **334**, 488–492.
- Stöckhert, B., Duyster, J., Trepmann, C., Massonne, H.J. (2001): Microdiamond daughter crystals precipitated from supercritical COH + silicate fluids included in garnet, Erzgebirge, Germany. *Geology*, **29**, 391–394.
- Suzuki, A. & Ohtani, E. (2003): Density of peridotite melts at high pressure. *Phys. Chem. Minerals*, **30**, 449–456.
- Terry, M.P. & Robinson, P. (2003): Evolution of amphibolite-facies structural features and boundary conditions for deformation during exhumation of high- and ultrahigh-pressure rocks, Nordøyane, Western Gneiss Region, Norway. *Tectonics*, **22**, 1036, 10.1029/2001TC001349.
- Torsvik, T.H., Smethurst, M.A., Meert, J.G., VanderVoo, R., McKerrow, W.S., Brasier, M.D., Sturt, B.A., Walderhaug, H.J. (1996): Continental break-up and collision in the Neoproterozoic and Palaeozoic – a tale of Baltica and Laurentia. *Earth Sci. Rev.*, **40**, 229–258.
- Trepmann, C. & Stöckhert, B. (2001): Mechanical twinning of jadeite – an indication of synseismic loading beneath the brittle-plastic transition. *Int. J. Earth Sci.*, **90**, 4–13.
- , — (2003): Quartz microstructures developed during non-steady state plastic flow at rapidly decaying stress and strain rate. *J. Struct. Geol.*, **25**, 2035–2051.
- Tucker, R.D., Robinson, P., Solli, A., Gee, D.G., Thorsnes, T., Krogh, T.E., Nordgulen, O., Bickford, M.E. (2004): Thrusting and extension in the Scandian hinterland, Norway: new U-Pb ages and tectonostratigraphic evidence. *Am. J. Sci.*, **304**, 477–532.
- Turcotte, D.L. & Schubert, G. (2002): *Geodynamics*. 2nd ed. Cambridge University Press, Cambridge, 456 p.
- van der Molen, I. & van Roermund, H.L.M. (1986): The pressure path of solid inclusions in minerals: the retention of coesite inclusions during uplift. *Lithos*, **19**, 317–324.
- Vrijmoed, J.C. (2008): Stop 10.1. Diamond-bearing Svartberget olivine-websterite. in “A tectonostratigraphic transect across the central Scandinavian Caledonides, Part II preliminary”, P. Robinson, D. Roberts, D. Gee., eds. NGU, Trondheim, 2–5.
- Vrijmoed, J.C., Van Roermund, H.L.M., Davies, G.R. (2006): Evidence for diamond-grade ultra-high pressure metamorphism and fluid interaction in the Svartberget Fe-Ti garnet peridotite-websterite body, Western Gneiss Region, Norway. *Mineral. Petrol.*, **88**, 381–405.
- Vrijmoed, J.C., Smith, D.C., van Roermund, H.L.M. (2008): Raman confirmation of microdiamond in the Svartberget Fe-Ti type garnet peridotite, Western Gneiss Region, Western Norway. *Terra Nova*, **20**, 295–301.
- Warren, C.J., Beaumont, C., Jamieson, R.A. (2008): Modelling tectonic styles and ultra-high pressure (UHP) rock exhumation during the transition from oceanic subduction to continental collision. *Earth Planet. Sci. Lett.*, **267**, 129–145.
- Wheeler, J. (1991): Structural evolution of a subducted continental sliver – the Northern Dora Maira Massif, Italian Alps. *J. Geol. Soc. Lond.*, **148**, 1101–1113.
- Ye, K., Liou, J.B., Cong, B., Maruyama, S. (2001): Overpressures induced by coesite-quartz transition in zircon. *Am. Mineral.*, **86**, 1151–1155.
- Zhang, Y. (1998): Mechanical and phase equilibria in inclusion-host systems. *Earth Planet. Sci. Lett.*, **157**, 209–222.

Received 13 January 2009

Modified version received 14 May 2009

Accepted 12 October 2009